Synthesis, Characterization, and Anticancer Activity of a Series of Ketone-N4-Substituted Thiosemicarbazones and Their Ruthenium(II) Arene Complexes

Wei Su,*[†,‡] Quanquan Qian,[†] Peiyuan Li,*[§] Xiaolin Lei,[†] Qi Xiao,[†] Shan Huang,[†] Chusheng Huang,[†] and Jianguo Cui[†]

[†]Key Laboratory of Beibu Gulf Environment Change and Resources Utilization (Guangxi Teachers Education University), Ministry of Education, Nanning, China

[‡]College of Chemistry and Life Science, Guangxi Teachers Education University, 175 Mingxiu East Road, Nanning 530000, China

[§]College of Pharmacy, Guangxi University of Traditional Medicine,179 Mingxiu East Road, Nanning, China

Ⓢ Supporting Information

ABSTRACT: A series of ketone-N4-substituted thiosemicarbazone (TSC) compounds (**L1−L9**) and their corresponding $[(\eta^6\text{-}p\text{-cymene})Ru^{II}(TSC)Cl]^{+/0}$ complexes (**1−9**) were synthesized and characterized by NMR, IR, elemental analysis, and HR-ESI-mass spectrometry. The molecular structures of **L4**, **L9**, **1−6**, and **9** were determined by single-crystal X-ray diffraction analysis. The compounds were further evaluated for their *in vitro* antiproliferative activities against the SGC-7901 human gastric cancer, BEL-7404 human liver cancer, and HEK-293T noncancerous cell lines. Furthermore, the interactions of the compounds with DNA were followed by electrophoretic mobility spectrometry studies.
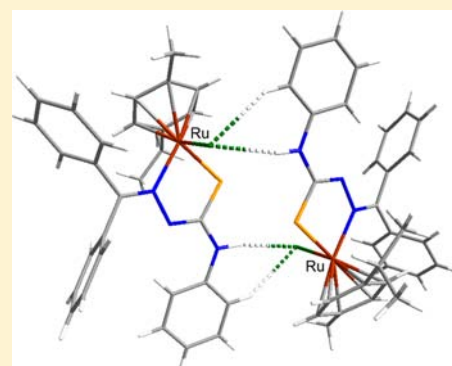
■ INTRODUCTION

Thiosemicarbazones (TSCs) have attracted considerable attention by chemists and biologists because of their wide range of pharmacological effects; these compounds and their metal complexes have shown marked antibacterial, antiviral, antifungal, and, particularly, antitumor activity.[1] In recent years, a number of TSC derivatives have been synthesized, and their antitumor activity against a broad spectrum of chemotherapeutic properties were also evaluated.[2] Moreover, the complexes consisted of transition metals, and TSC ligands usually possess more potent pharmacological effects than the thiosemicarbazone ligands alone.[3] The biological properties of the TSC ligands can be modified and improved by the linkage to transition metal ions.[4]

The ruthenium-based complexes, which exhibit considerable promise in antiproliferation activity and lower toxicity than platinum drugs,[5] have been developed in the last two decades. In particular, the Ru(III) complexes, [HIm][trans-RuCl$_4$(DMSO)(Im)] (NAMI-A) and [ImH][trans-Ru-Cl$_4$(Im)$_2$] (KP1019), have progressed into clinical trials with very promising results.[6] The organometallic Ru(II) arene complexes, with the half-sandwich type structure, have demonstrated their potential increasingly.[7] Their coordination sites can be filled with various ligands, which offer numerous possibilities to modulate biological and pharmacological properties by proper ligand selection.[8] For instance, Ru(II)

arene complexes with ethylenediamine (en) as the ligand can bind to DNA and thus lead to cytotoxicity toward cancer cells.[9] In addition, related complexes incorporating the 1,3,5-triaza-7-phosphatricyclo-[3.3.1.1]-decane (PTA) ligand, e.g., $[(\eta^6\text{-}p\text{-}cymene)Ru^{II}(PTA)Cl_2]$ (RAPTA-C), showed activity against metastases.[10]

The Ru(II)-arene complexes of TSCs have also emerged as an approach to develop promising lead Ru-based therapeutic agents. Beckford et al. reported the first structurally characterized ruthenium-arene half-sandwich complexes with thiosemicarbazone ligands combining the $\{(\eta^6\text{-}p\text{-cymene})Ru^{II}\}$ moiety with 9-anthracenyl-TSC derivatives as ligands.[4a] These complexes exhibited good cytotoxic profiles against different human cancer cell lines, and their biological activities were apparently modulated by the TSC coligand.[11] More recently, Smith et al. demonstrated the cytotoxicity and antiparasitic activity of a set of TSC derivatives and their corresponding Ru(II)-arene complexes.[12] Moreover, the pharmacological activity of the binuclear TSC Ru-arene complexes were also demonstrated by Gambino and his co-workers.[13]

Although the TSC Ru-arene complexes have been proven to have potential as effective anticancer drugs, their distinct modes of action and biological targets are still the focus of active

research. In this Article, a series of TSC derivatives (**L1–L9**) and their corresponding Ru(II)-arene complexes (**1–9**) were synthesized and characterized. The cytotoxicity toward the SGC-7901 human gastric and BEL-7404 human liver cancer cell lines of these compounds was investigated. In addition, the interactions of the compounds with DNA were followed by electrophoretic mobility spectrometry studies.

■ EXPERIMENTAL SECTION

Materials. The starting material $[(\eta^6\text{-}p\text{-cymene})RuCl_2]_2$ was prepared according to literature methods.[11]

General Procedure for the Synthesis of Thiosemicarbazones. All of the thiosemicarbazones were prepared by previously reported procedures.[11] The relevant thiosemicarabazide (1 mmol) and ketone (1 mmol) were combined in methanol (5 mL) with acetic acid (1–2 drops). The mixture was refluxed for 3 h, during which a white or off-white precipitate appeared. After 3 h, the mixture was allowed to cool to room temperature, and dried in vacuo. Ligands were further purified by recrystalliztion from methanol. HR-ESI-MS and ¹H NMR data were collected for all ligands.

General Procedure for the Synthesis of $[(\eta^6\text{-}p\text{-Cymene})\text{-}Ru^{II}(TSC)Cl]^{+/0}$ Complexes. The $[(\eta^6\text{-}p\text{-cymene})Ru^{II}(TSC)Cl]Cl$ complexes were obtained by reacting the dimer $[(\eta^6\text{-}p\text{-cymene})\text{-}RuCl_2]_2$ and the thiosemicarbazone ligands.[7] Thiosemicarbazone (0.1 mmol) and $[(\eta^6\text{-}p\text{-cymene})RuCl_2]_2$ (0.05 mmol) were combined in acetone (8 mL). The resultant mixture was stirred and refluxed. After 3 h, the mixture was allowed to cool to room temperature, and the dark solid formed was filtered. All metal complexes were subsequently purified by recrystallization from ethanol and hexane. HR-ESI-MS, IR, ¹H NMR (300 MHz, CDCl₃), and elemental analysis were performed for all metal complexes.

Characterization Data. *[(η⁶-p-Cymene)Ruᴵᴵ(L1)Cl]Cl (1).* Yield: 20 mg (44%). HR-ESI-MS (MeOH) *m/z* [Found (Calcd)]: 366.0581 (366.0581) (100%) $\{[(\eta^6\text{-cymene})Ru(\mathbf{L1})Cl] - HCl\}^+$. IR (cm⁻¹): ν (NH₂, NH) 3432, 3252, 3190; ν (C=N) 1621; ν (C=S) 1045. UV−vis (methanol) λ: 306, 264, 229 nm. ¹H NMR (300 MHz, CDCl₃) δ: 13.336 (br, 1H, NH), 9.390 (br, 1H, NH₂), 6.488 (br, 1H, NH₂), 5.664 (d, 1H, p-cym phenyl-*H*, J = 6.1 Hz), 5.539 (q, 2H, p-cym phenyl-*H*, J = 6.2 Hz), 5.386 (d, 1H, p-cym phenyl-*H*, J = 6.1 Hz), 2.905−2.813 (m, 1H, p-cym C*H*(CH₃)₂), 2.855 (s, 3H, C(C*H₃*)₂), 2.660 (s, 3H, C(C*H₃*)₂), 2.274 (s, 3H, p-cym CC*H₃*), 1.301 (d, 3H, p-cym CH(C*H₃*)₂, J = 7.0 Hz), 1.238 (d, 3H, p-cym CH(C*H₃*)₂, J = 7.0 Hz) ppm. Anal. Calcd for C₁₄H₂₂Cl₂N₃RuS·H₂O: C, 37.00; H, 5.32; N, 9.25. Found: C, 37.1; H, 5.55; N, 9.24. Single crystals suitable for X-ray diffraction were obtained by recrystallization in ethanol and hexane (30/70) solution.

[(η⁶-p-Cymene)Ruᴵᴵ(L2)Cl]Cl (2). Yield 20 mg,(43%). HR-ESI-MS (MeOH) *m/z* [Found (Calcd)]: 380.0737 (380.0738) (100%) $\{[(\eta^6\text{-}p\text{-cymene})Ru(\mathbf{L2})Cl] - HCl\}^+$. IR (cm⁻¹): ν (NH₂, NH) 3452; ν (C=N) 1625; ν (C=S) 1086. UV−vis (methanol) λ: 263, 230 nm. ¹H NMR (300 MHz, CDCl₃) δ: 12.789 (br, 1H, NH), 9.842 (br, 1H, NH), 5.657 (d, 1H, p-cym phenyl-*H*, J = 6.0 Hz), 5.513 (s, 2H, p-cym phenyl-*H*), 5.398 (d, 1H, p-cym phenyl-*H*, J = 6.0 Hz), 3.154 (d, 3H, NHC*H₃*, J = 4.9 Hz), 2.883−2.791 (m, 1H, p-cym C*H*(CH₃)₂), 2.834 (s, 3H, C(C*H₃*)₂), 2.618 (s, 3H, C(C*H₃*)₂), 2.258 (s, 3H, p-cym CC*H₃*), 1.288 (d, 3H, p-cym CH(C*H₃*)₂, J = 7.0 Hz), 1.219 (d, 3H, p-cym CH(C*H₃*)₂, J = 7.0 Hz) ppm. Anal. Calcd for C₁₅H₂₃Cl₂N₃RuS·0.5H₂O: C, 39.13; H, 5.69; N, 9.13. Found: C, 39.23; H, 5.56; N, 9.42. Single crystals suitable for X-ray diffraction were obtained by recrystallization in ethanol and hexane (30/70) solution.

[(η⁶-p-Cymene)Ruᴵᴵ(L3)Cl]Cl (3). Yield 30 mg (57%). HR-ESI-MS (MeOH) *m/z* [Found (Calcd)]: 442.0900 (442.0896) (100%) $\{[(\eta^6\text{-}p\text{-cymene})Ru(\mathbf{L3})Cl] - HCl\}^+$. IR (cm⁻¹): ν (NH₂, NH) 3432; ν (C=N) 1642; ν (C=S) 1057. UV−vis (methanol) λ: 278, 230 nm. ¹H NMR (300 MHz, CDCl₃) δ: 13.260 (br, 1H, NH), 11.851 (br, 1H, NH), 7.576 (d, 2H, phenyl-*H*, J = 8.0 Hz), 7.421 (t, 2H, phenyl-*H*, J = 7.7 Hz), 7.321 (d, 1H, phenyl-*H*, J = 7.4 Hz), 5.618 (d, 1H, p-cym phenyl-*H*, J = 5.8 Hz), 5.529 (s, 2H, p-cym phenyl-*H*), 5.374 (d, 1H, p-cym phenyl-*H*, J = 5.9 Hz), 2.842−2.773 (m, 1H, p-cym CH(CH₃)₂),

2.890 (s, 3H, C(C*H₃*)₂), 2.708 (s, 3H, C(C*H₃*)₂), 2.267 (s, 3H, p-cym CC*H₃*), 1.269 (d, 3H, p-cym CH(C*H₃*)₂, J = 6.9 Hz), 1.222 (d, 3H, p-cym CH(C*H₃*)₂, J = 6.9 Hz) ppm. Anal. Calcd for C₂₀H₂₇Cl₂N₃RuS·0.5H₂O: C, 45.97; H, 5.40; N, 8.04. Found: C, 46.24; H, 5.24; N, 8.09. Single crystals suitable for X-ray diffraction were obtained by recrystallization in ethanol and hexane (30/70) solution.

[(η⁶-p-Cymene)Ruᴵᴵ(L4)Cl]Cl (4). Yield 25.5 mg, (51%). HR-ESI-MS (MeOH) *m/z* [Found (Calcd)]: 428.0740 (428.0739) (100%) $\{[(\eta^6\text{-}p\text{-cymene})Ru(\mathbf{L4})Cl] - HCl\}^+$. IR (cm⁻¹): ν (NH₂, NH) 3436, 3256; ν (C=N) 1613; ν (C=S) 1025. UV−vis (methanol) λ: 231 nm. ¹H NMR (300 MHz, CDCl₃) δ: 7.96 (br, 2H, NH₂), 7.50 (m, 3H, C-phenyl), 7.30 (br, 1H, NH), 7.24 (m, 2H, C-phenyl), 5.41 (d, 1H, p-cym, J = 5.7 Hz), 4.94 (d, 1H, p-cym, J = 5.7 Hz), 4.74 (d, 1H, p-cym, J = 5.7 Hz), 4.63 (d, 1H, p-cym, J = 5.7 Hz), 3.70 (m, 3H, CNCH₃), 2.82−2.73 (m, 1H, p-cym C*H*(CH₃)₂), 2.03 (s, 3H, p-cym CC*H₃*), 1.25 (d, 3H, p-cym CH(C*H₃*)₂, J = 6.9 Hz), 1.18 (d, 3H, p-cym CH(C*H₃*)₂, J = 6.9 Hz) ppm. Anal. Calcd for C₁₉H₂₅Cl₂N₃RuS·0.5H₂O: C, 44.88; H, 5.15; N, 8.26. Found: C, 45.15; H, 5.02; N, 8.24. Single crystals suitable for X-ray diffraction were obtained by recrystallization in chloroform and hexane (30/70) solution.

[(η⁶-p-Cymene)Ruᴵᴵ(L5)Cl]Cl (5). Yield 30 mg (58%). HR-ESI-MS (MeOH) *m/z* [Found (Calcd)]: 442.1096 (442.0896) (100%) $\{[(\eta^6\text{-}p\text{-cymene})Ru(\mathbf{L5})Cl] - HCl\}^+$. IR (cm⁻¹): ν (NH₂, NH) 3444, 3182, 3117; ν (C=N) 1593; ν (C=S) 1037. UV−vis (methanol) λ: 342, 266, 230 nm. ¹H NMR (300 MHz, CDCl₃) δ: 12.62 (br, 1H, NNH), 10.31 (br, 1H, NHCH₃), 7.89 (s, 2H, C-phenyl), 7.60 (d, 3H, C-phenyl), 5.29 (d, 1H, p-cym, J = 5.7 Hz), 4.91 (d, 1H, p-cym, J = 5.7 Hz), 4.67 (d, 1H, p-cym, J = 5.7 Hz), 3.85 (d, 1H, p-cym, J = 5.7 Hz), 3.18 (d, 3H, NHCH₃, J = 3.6 Hz), 2.95 (m, 3H, CNCH₃), 2.69−2.62 (m, 1H, p-cym C*H*(CH₃)₂), 2.02 (s, 3H, p-cym CC*H₃*), 1.16 (d, 3H, p-cym CH(C*H₃*)₂, J = 6.9 Hz), 1.11 (d, 3H, p-cym CH(C*H₃*)₂, J = 6.9 Hz) ppm. Anal. Calcd for C₂₀H₂₇Cl₂N₃RuS·0.75CH₂Cl₂: C, 43.18; H, 4.98; N, 7.28. Found: C, 42.76; H, 4.84; N, 7.29. Single crystals suitable for X-ray diffraction were obtained by recrystallization in chloroform and hexane (30/70) solution.

[(η⁶-p-Cymene)Ruᴵᴵ(L6)Cl]Cl (6). Yield 30 mg (51%). HR-ESI-MS (MeOH) *m/z* [Found (Calcd)]: 504.1038 (504.1053) (100%) $\{[(\eta^6\text{-}p\text{-cymene})Ru(\mathbf{L6})Cl] - HCl\}^+$. IR (cm⁻¹): ν (NH₂, NH) 3440, 3256, 3137; ν (C=N) 1621; ν (C=S) 1025. UV−vis (methanol) λ: 273, 229 nm. ¹H NMR (300 MHz, CDCl₃) δ: 13.005 (br, 1H, NH), 12.349 (br, 1H, NH), 7.917 (s, 2H, phenyl-*H*), 7.648−7.623 (m, 5H, phenyl-*H*), 7.440−7.389 (m, 2H, phenyl-*H*), 7.316−7.291 (m, 1H, phenyl-*H*), 5.249 (d, 1H, p-cym phenyl-*H*, J = 5.7 Hz), 4.914 (d, 1H, p-cym phenyl-*H*, J = 5.7 Hz), 4.646 (d, 1H, p-cym phenyl-*H*, J = 5.7 Hz), 3.910 (d, 1H, p-cym phenyl-*H*, J = 5.7 Hz), 3.043 (s, 3H, CC*H₃*), 2.698−2.591 (m, 1H, p-cym C*H*(CH₃)₂), 2.022 (s, 3H, p-cym CC*H₃*), 1.162−1.112 (m, 6H, p-cym CH(C*H₃*)₂) ppm. Anal. Calcd for C₂₅H₂₉Cl₂N₃RuS·1.5CH₂Cl₂: C, 45.28; H, 4.59; N, 5.98. Found: C, 45.53; H, 4.44; N, 6.12. Single crystals suitable for X-ray diffraction were obtained by recrystallization in chloroform and hexane (30/70) solution.

[(η⁶-p-Cymene)Ruᴵᴵ(L7)Cl]Cl (7). Yield 36 mg, (63%). HR-ESI-MS (MeOH) *m/z* [Found (Calcd)]: 490.0897 (490.0897) (100%) $\{[(\eta^6\text{-}p\text{-cymene})Ru(\mathbf{L7})Cl] - HCl\}^+$. IR (cm⁻¹): ν (NH₂, NH) 3448, 3256, 3051; ν (C=N) 1621; ν (C=S) 1123. UV−vis (methanol) λ: 303, 229 nm. ¹H NMR (300 MHz, CDCl₃) δ: 8.858 (br, 1H, NH), 8.767 (br, 1H, NH₂), 7.884 (br, 1H, NH₂), 7.616−7.293 (m, 10H, phenyl-*H*), 5.385 (d, 1H, p-cym phenyl-*H*, J = 5.8 Hz), 5.024 (d, 1H, p-cym phenyl-*H*, J = 5.8 Hz), 4.778 (d, 1H, p-cym phenyl-*H*, J = 5.8 Hz), 3.857 (d, 1H, p-cym phenyl-*H*, J = 5.8 Hz), 3.035−2.966 (m, 1H, C*H*(CH₃)₂), 2.238 (s, 3H, p-cym CC*H₃*), 1.322 (d, 6H, p-cym CH(C*H₃*)₂, J = 6.9 Hz) ppm. Anal. Calcd for C₂₄H₂₇Cl₂N₃RuS·0.5H₂O: C, 50.52; H, 4.95; N, 7.37. Found: C, 50.51; H, 4.91; N, 7.29.

[(η⁶-p-Cymene)Ruᴵᴵ(L8)Cl]Cl (8). Yield 29.5 mg (50%). HR-ESI-MS (MeOH) *m/z* [Found (Calcd)]: 504.1065 (504.1053) (100%) $\{[(\eta^6\text{-}p\text{-cymene})Ru(\mathbf{L8})Cl] - HCl\}^+$. IR (cm⁻¹): ν (NH₂, NH) 3450; ν (C=N) 1634; ν (C=S) 1070. UV−vis (methanol) λ: 360, 231 nm. ¹H NMR (300 MHz, CDCl₃) δ: 12.364 (br, 1H, NH), 10.560 (br, 1H, NH), 7.881 (s, 2H, phenyl-*H*), 7.758−7.527 (m, 6H, phenyl-*H*), 7.307−7.295 (m, 2H, phenyl-*H*), 5.371 (d, 1H, p-cym phenyl-*H*, J =

Table 1. Crystal Data and Details of Data Collection for L4, L9, 1–6, and 9

	L4	L9	1	2	3	4	5·CHCl₃	6·CHCl₃	9
formula	$C_9H_{11}N_3S$	$C_{20}H_{17}N_3S$	$C_{14}H_{22}Cl_2N_3RuS$	$C_{15}H_{25}Cl_2N_3RuS$	$C_{20}H_{27}Cl_2N_3RuS$	$C_{19}H_{25}Cl_2N_3RuS$	$C_{21}H_{28}Cl_5N_3RuS$	$C_{26}H_{30}Cl_5N_3RuS$	$C_{30}H_{30}ClN_3RuS$
M_r	193.27	331.43	436.38	451.41	513.48	499.02	630.95	692.96	601.09
cryst syst	monoclinic	monoclinic	monoclinic	triclinic	triclinic	triclinic	triclinic	triclinic	monoclinic
space group	$P2/n$	$P2_1/c$	$P2_1/c$	$P\bar{1}$	$P\bar{1}$	$P\bar{1}$	$P\bar{1}$	$P\bar{1}$	$P2_1/n$
a (Å)	15.2988(14)	5.6023(3)	15.0058(4)	9.1282(5)	9.8347(4)	9.5604(4)	9.9135(5)	9.9199(4)	10.4360(4)
b (Å)	5.8431(4)	10.2081(4)	9.1451(2)	10.8602(6)	10.3501(6)	10.2639(4)	11.8264(5)	11.3989(5)	18.1288(6)
c (Å)	25.917(2)	29.8821(12)	14.6149(4)	11.0433(6)	12.0090(5)	11.8418(5)	12.9485(5)	13.7623(5)	14.6373(5)
α (deg)	90	90	90	92.243(5)	76.142(4)	93.671(3)	106.537(4)	90.441(3)	90.00
β (deg)	97.044(9)	92.960(4)	112.668(3)°	102.438(5)	71.965(4)	110.623(4)	102.353(4)	104.198(3)	96.078(3)
γ (deg)	90	90	90	114.849(5)	84.612(4)	99.169(3)	107.465(4)	94.091(4)	90.00
V (Å³)	2299.3(3)	1706.64(14)	1850.67(10)	959.67(9)	1128.24(9)	1064.53(7)	1311.71(10)	1504.31(11)	2753.68(16)
Z	4	4	4	2	2	2	2	2	4
D_{calcd} (Mg/m³)	1.209	1.29	1.5661	1.562	1.511	1.481	1.532	1.469	1.378
$F(000)$	880	696	884.0	460	524	459	585	645	1113
μ (mm⁻¹)	0.255	0.195	1.25	1.204	1.034	1.091	1.199	1.053	0.763
R_{int}	0.0201	0.0215	0.0228	0.0466	0.0301	0.0297	0.0392	0.0300	0.0323
θ range (deg)	6.34–52.74	6.76–52.74	5.95–50	5.82–52.72	5.88–52.74	5.54–52.74	5.84–52.74	5.66–52.74	6.42–52.74
reflns collected	10231	8565	7084	7909	9294	9070	10993	15 287	16447
ind reflns	4695	3471	3239	3908	4594	4339	5379	6160	5614
GOF (S)	1.059	1.077	1.069	1.060	1.056	1.041	1.036	1.035	1.044
R1/wR2 [$I \geq 2\sigma(I)$]	0.0643/0.1804	0.0496/0.1150	0.0341/0.0870	0.0343/0.0750	0.0353/0.0707	0.0356/0.0764	0.0441/0.0809	0.0382/0.0850	0.0318/0.0706
R1/wR2 (all data)	0.087/0.2022	0.0668/0.1267	0.0445/0.0870	0.0429/0.0832	0.0439/0.0772	0.0453/0.0823	0.0583/0.0922	0.0483/0.0909	0.0452/0.0762

Table 2. Selected Bond Lengths (Å) and Angles (deg) in L4, L9, 1−6, and 9

	L4	L9	1	2	3	4	5·CHCl$_3$	6·CHCl$_3$	9
C11−S1	1.6822(29)	1.6589(21)	1.7001(45)	1.7025(38)	1.6983(30)	1.6869(34)	1.6957(36)	1.6877(29)	1.7347(26)
C11−N1	1.3143(43)	1.3416(26)	1.3166(68)	1.3301(39)	1.3302(42)	1.3245(41)	1.3101(63)	1.3436(41)	1.3694(30)
C11−N2	1.3489(37)	1.3677(25)	1.3360(48)	1.3362(54)	1.3432(36)	1.3415(48)	1.3469(48)	1.3479(41)	1.3015(32)
N2−N3	1.3828(33)	1.3688(24)	1.3961(45)	1.4033(32)	1.3949(33)	1.4060(32)	1.3973(45)	1.3918(34)	1.4092(26)
Ru1−centroid			1.6935(3)	1.6958(2)	1.6950(3)	1.6968(2)	1.6864(3)	1.6964(2)	1.6976(2)
Ru1−S1			2.3696(15)	2.3727(10)	2.3727(8)	2.3511(9)	2.3512(12)	2.3405(9)	2.3355(6)
Ru1−Cl1			2.3984(12)	2.4147(8)	2.3978(11)	2.4116(9)	2.4056(13)	2.4067(8)	2.4351(8)
Ru1−N3			2.1307(31)	2.1274(28)	2.1356(20)	2.1633(23)	2.1587(22)	2.1452(25)	2.1240(19)
N3−Ru1−S1			80.548(86)	80.963(68)	80.408(62)	82.427(71)	81.484(88)	81.916(65)	81.266(51)
S1−Ru1−Cl1			86.700(42)	88.398(32)	87.703(30)	86.704(31)	86.225(41)	88.308(30)	87.809(26)
Cl1−Ru1−N3			87.861(79)	86.159(83)	87.937(81)	85.768(63)	89.868(89)	84.807(82)	83.667(54)

5.7 Hz), 5.026 (d, 1H, *p*-cym phenyl-*H*, *J* = 5.7 Hz), 4.749 (d, 1H, *p*-cym phenyl-*H*, *J* = 5.7 Hz), 3.867 (d, 1H, *p*-cym phenyl-*H*, *J* = 5.7 Hz), 3.096 (d, 3H, NHC*H*$_3$, *J* = 4.2 Hz), 2.800−2.754 (m, 1H, *p*-cym C*H*(CH$_3$)$_2$), 2.085 (s, 3H, *p*-cym CC*H*$_3$), 1.263−1.214 (m, 6H, *p*-cym CH(C*H*$_3$)$_2$) ppm. Anal. Calcd for C$_{25}$H$_{29}$Cl$_2$N$_3$RuS·H$_2$O: C, 50.59; H, 5.26; N, 7.08. Found: C, 50.66; H, 5.04; N, 7.08.

[(η^6-*p*-Cymene)Ru^{II}(L9)Cl] (9). Yield 35 mg (54%). HR-ESI-MS (MeOH) *m*/*z* [Found (Calcd)]: 566.1226 (566.1212) (100%) {[(η^6-*p*-cymene)Ru(**L9**)Cl] − Cl}$^+$. IR (cm^{-1}): ν (NH$_2$, NH) 3450, 3264; ν (C=N) 1650; ν (C=S) 1050. UV−vis (methanol) λ: 335, 251, 228 nm. ^{1}H NMR (300 MHz, CDCl$_3$) δ: 8.082 (br, 1H, NH), 7.549−7.517 (m, 3H, phenyl-*H*), 7.417−7.334 (m, 3H, phenyl-*H*), 7.296−7.265 (m, 3H, phenyl-*H*), 6.982−6.884 (m, 4H, phenyl-*H*), 6.803−6.706 (m, 2H, phenyl-*H*), 5.437 (d, 1H, *p*-cym phenyl-*H*, *J* = 6.0 Hz), 4.974 (d, 1H, *p*-cym phenyl-*H*, *J* = 6.0 Hz), 4.727 (d, 1H, *p*-cym phenyl-*H*, *J* = 6.0 Hz), 3.842 (d, 1H, *p*-cym phenyl-*H*, *J* = 6.0 Hz), 2.813−2.720 (m, 1H, *p*-cym C*H*(CH$_3$)$_2$), 2.080 (s, 3H, *p*-cym CC*H*$_3$), 1.193 (d, 3H, *p*-cym CH(C*H*$_3$)$_2$, *J* = 6.9 Hz), 1.152 (d, 3H, *p*-cym CH(C*H*$_3$)$_2$, *J* = 6.9 Hz) ppm. Anal. Calcd for C$_{30}$H$_{31}$Cl$_2$N$_3$RuS·3CH$_2$Cl$_2$: C, 49.25; H, 5.13; N, 6.89. Found: C, 49.42; H, 5.14; N, 6.75. Single crystals suitable for X-ray diffraction were obtained by recrystallization in chloroform and hexane (30/70) solution.

Methods and Instrumentantion. NMR spectra were recorded on a Bruker AV-300 spectrometer at working frequency 300 MHz. Chemical shifts are expressed in parts per million (δ) values and coupling constants (*J*) in Hertz. Mass spectra for the complexes were recorded on a Waters UPLC XEVO G2 TOF mass spectrometer using electrospray ionization probe. Elemental analyses were carried out using an Elementar Vario EL Cube.

X-ray Crystallographic Determination. All reflection data were collected on a Bruker SMART CCD instrument by using graphite monochromatic Mo Kα radiation (λ = 0.710 73 Å) at room temperature. A semiempirical absorption correction by using the SADABS program was applied, and the raw data frame integration was performed with SAINT.[14] The crystal structures were solved by the direct method using the program SHELXS-97[15] and refined by the full-matrix least-squares method on F^2 for all non-hydrogen atoms using SHELXTL-97[16] with anisotropic thermal parameters. All hydrogen atoms were located in calculated positions and refined isotropically, except that the hydrogen atoms of water molecules were fixed in a difference Fourier map and refined isotropically. The details of the crystal data were summarized in Table 1, and selected bond lengths and angles for **L4**, **L9**, **1−6**, and **9** are listed in Table 2. Crystallographic data for the structural analysis have been deposited with the Cambridge Crystallographic Data Center. CCDC reference numbers follow: 941661 (**L4**), 941662 (**L9**), 860112 (**1**), 883966 (**2**), 860113 (**3**), 884189 (**4**), 941658 (**5**), 941659 (**6**), 941660 (**9**).

Cell Culture and Assay for Cell Viability. SGC-7901 (gastric carcinoma), BEL-7404 (liver carcinoma), and HEK-293T (human embryonic kidney) cell lines. Cells were obtained by Commerce. Cells were grown in RPMI-1640 supplemented with 10% cosmic calf serum (Hyclone) and antibiotics in a humidified atmosphere of 5% CO$_2$ at 37 °C. The viability of these cells was determined using the colorimetric Cell Titer 96 aqueous cell proliferation assay (MTT) according to the instructions provided by the manufacturer (Promega, Madison, WI). Briefly, cells (1−3 × 10^4 cells per well) were seeded in 96 wells plates. One day after seeding, the cells were treated with or without a different concentration of each compound and reincubated for 72 h. After the cells were washed with sterile phosphate buffer saline (PBS), 190 µL of RPMI-1640 and 10 µL of the tetrazolium dye (MTT) (5 mg/mL) solution were added to each well, and the cells were incubated for an additional 4 h. The medium was discarded; 200 µL of DMSO was added to dissolve the purple formazan crystals formed. The absorbance (A) at 492 nm was measured using a Thermo Scientific Multiskan MK3.

DNA Cleavage Studies Using Agarose Gel Electrophoresis. In the gel electrophoresis experiments, supercoiled plasmid pB*R*322 DNA was treated with compound, and the mixture was incubated for 30 min at 37 °C. The samples were then analyzed by 1.5% agarose gel electrophoresis in Tris−acetic acid−ethylenediamine tetraacetic acid buffer. The gel was stained with 0.5 µg mL^{-1} ethidium bromide before migration. After electrophoresis at 50 V for 3 h, the gel was illuminated, and the digital images were analyzed by gel documentation system (Junyi-Dongfang Co., JY02G).

RESULTS AND DISCUSSION

Synthesis and Characterization. For the study at hand, a series of ketone-N^4-substitued thiosemicarbazones (TSCs) and their corresponding [(η^6-*p*-cymene)Ru^{II}(TSC)Cl]$^{+/0}$ complexes were synthesized. The thiosemicarbazone ligands **L1−L9** were synthesized via the typical condensation route from their parent thiosemicarbazides and the appropriate ketone. Subsequently, the [(η^6-*p*-cymene)Ru^{II}(TSC)Cl]$^{+/0}$ complexes **1−9** were prepared via heating of the TSC ligands with [(η^6-*p*-cymene)RuCl$_2$]$_2$ (Figure 1).[11] The ligands **L1−L9** were characterized by ^{1}HNMR and HR-ESI-MS, and the complexes **1−9** were characterized with IR, HR-ESI-MS, and elemental analysis.

The ^{1}H NMR spectra of **L1−L9** display the broad peaks due to the imine protons in the range 6.29−9.50 ppm. There is a distinct shift in the imine proton for the metalloadducts **1−9** in comparison with the free proligand **L1−L9**, demonstrating the coordination of ruthenium to the ligands. The asymmetry (C_1) of the complexes induces significant modifications to the ^{1}H NMR signals of the *p*-cymene moiety in **1−9**. The ^{1}H NMR spectra of **1−9** in CDCl$_3$ show a doublet for each of the four *p*-cymene ring protons and two doublets for the methyl groups of the isopropyl moiety. The four proton resonances attributable to the *p*-cymene ring of **1−9** in CDCl$_3$ are in the range 3.82−5.67 ppm. In **1−3**, just as shown in Figure 2A, the four proton resonances attributable to the *p*-cymene ring are in the range 5.67−5.31 ppm. However, in **4−9**, just as shown in Figure 2B,C, one of the four proton resonances attributable to the *p*-

TSCs L1-L9
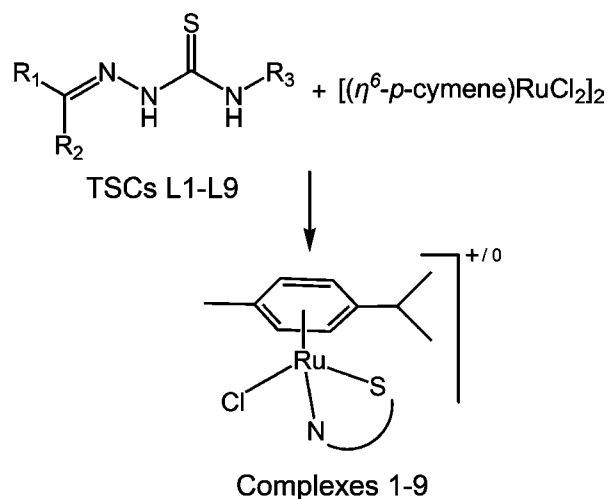
Complexes 1-9

TSC	Complex	R1	R2	R3
L1	1	Me	Me	H
L2	2	Me	Me	Me
L3	3	Me	Me	Ph
L4	4	Ph	Me	H
L5	5	Ph	Me	Me
L6	6	Ph	Me	Ph
L7	7	Ph	Ph	H
L8	8	Ph	Ph	Me
L9	9	Ph	Ph	Ph

Figure 1. General synthetic route to the TSCs and corresponding $[(\eta^6\text{-}p\text{-cymene})Ru^{II}(TSC)Cl]^{+/0}$ complexes.
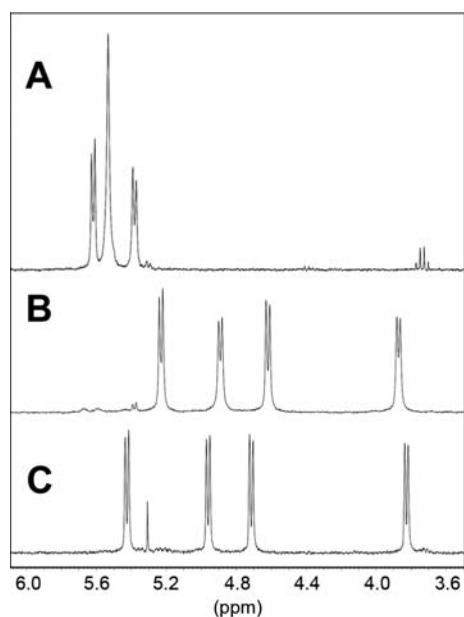

Figure 2. ^{1}H NMR spectra of **3** (A), **6** (B), and **9** (C) in CDCl$_3$ in the range 3.5−6.1 ppm.

cymene ring is strongly shifted to higher fields in the range 3.82−3.92 ppm, whereas the other three doublets are in the

range 4.63−5.39 ppm, indicating that it is typical of ruthenium arene systems.[17] The aforementioned high-field shift of one of the aromatic protons is likely due to the close vicinity of the phenyl group in the relevant ketone moiety of the coordinated ligand, as is confirmed by X-ray diffraction studies (see below).[18]

The X-ray crystal structures of acetone thiosemicarbazone (**L1**), acetone-N^4-methyl- thiosemicarbazone (**L2**), acetone-N^4-phenylthiosemicarbazone (**L3**), acetophenone-N^4- methylthio-semicarbazone (**L5**), acetophenone-N^4-phenylthiosemicarbazone (**L6**), and benzophenone thiosemicarbazone (**L7**) are known.[19] Herein, we have determined the structures of the remaining ligands from our series, namely acetophenone thiosemicarbazone (**L4**) and benzophenone-N^4-phenylthiosemicarbazone (**L9**) (Figure 3), with the crystals data being
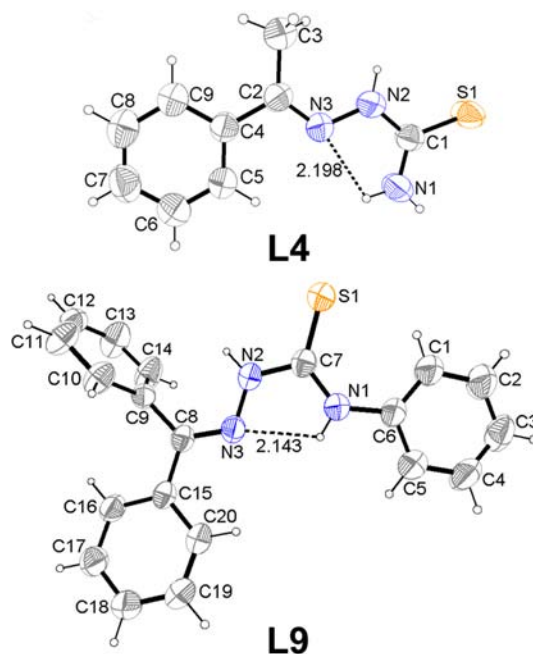

Figure 3. ORTEP plots of TSC ligands **L4** and **L9**; thermal ellipsoids are drawn at 50% probability.

presented in Table 1 and the selected bond lengths (Å) and angles (deg) being presented in Table 2. The structures of **L4** and **L9** are solved in the monoclinic space group $P2/n$ and $P2_1/c$, respectively. The pairs of donor atoms, N2 and S1, in an anti orientation are observed. The C11−S1 bonds, with the length of 1.659−1.682 Å, are typical of double bonds; that is, the thioamide tautomer is present.[20] The intramolecular H-bonds (N1−H···N3), 2.198 Å for **L4** and 2.143 Å for **L9**, are also noted.

The X-ray crystal structures of the Ru-arene complexes **1**, **2**, **3**, **4**, **5**, **6**, and **9** were also determined. Their structures and atom numbering schemes are shown in Figure 4. The crystallographic data are listed in Table 1, and selected bond lengths and angles are presented in Table 2. In all the complexes, Ru^{II} adopts the familiar "three-legged piano-stool" geometry with the metal center being coordinated by the aromatic arene ligand, a terminal chloride, and a chelating N,S-ligand. In all complexes, the arene ligands are essentially planar, and the distances between the ruthenium atom and the centroid of the aromatic ring of the arene ligand are in the range 1.686−1.698 Å. The molecular structures of complexes
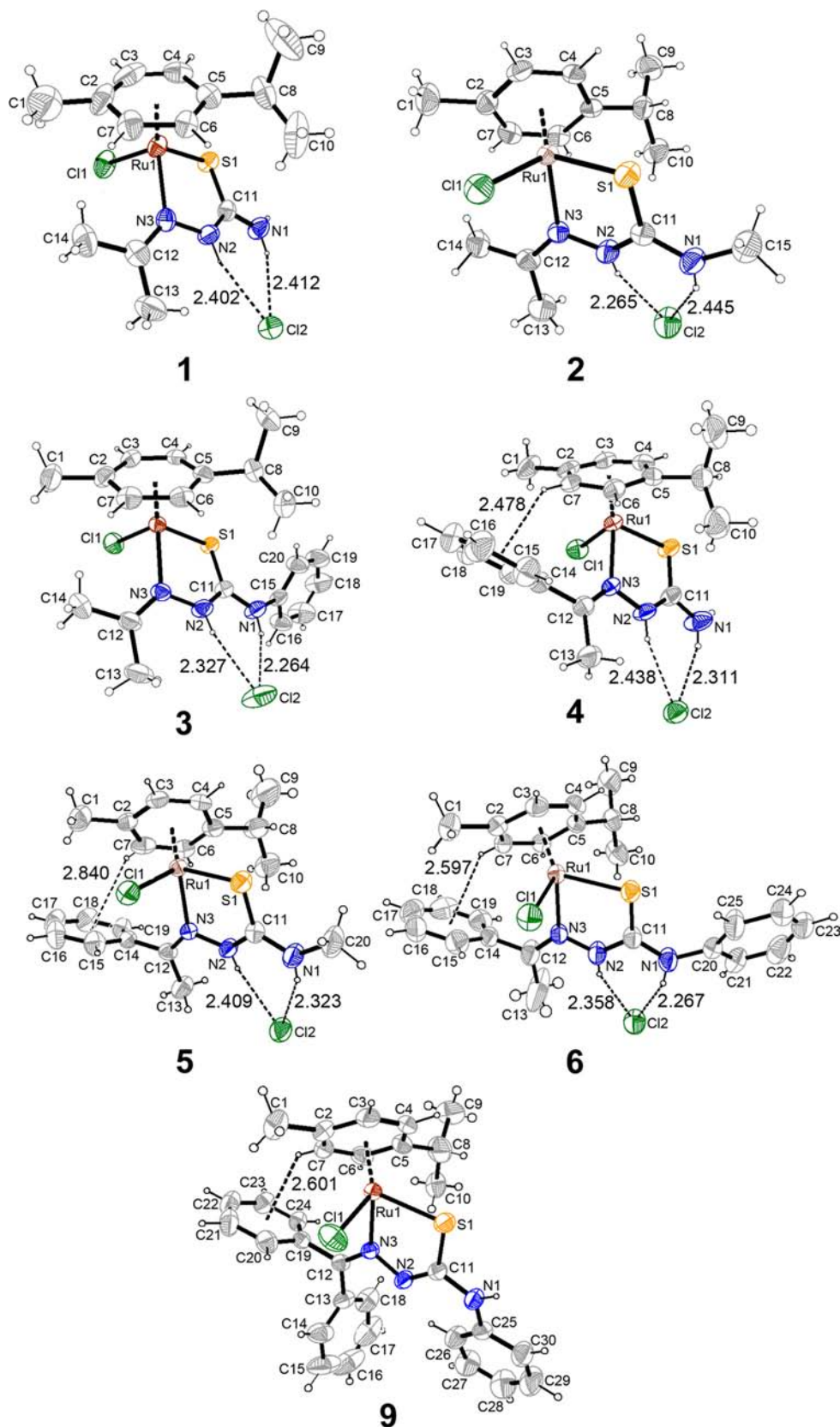
Figure 4. ORTEP plots of complex **1−6** and **9**; thermal ellipsoids are drawn at 50% probability. The solvent molecules have been omitted for clarity.

1−6 are similar. The bond distances around the Ru atom vary over a small range (Ru−S = 2.341−2.373 Å; Ru−N = 2.127−2.163 Å; Ru−Cl = 2.398−2.415 Å), which are comparable to those of similar compounds.[7] The Cl component of the anion are interlinked by N1−H···Cl2 (2.264−2.445 Å) and N2−H··· Cl2 (2.265−2.438 Å) hydrogen bonding interactions.

In the crystal structure of $[(\eta^6\text{-}p\text{-cymene})Ru^{II}(L1)Cl]Cl$ (**1**), an intramolecular hydrogen bond is formed between the

12445

dx.doi.org/10.1021/ic401362s | *Inorg. Chem.* 2013, 52, 12440−12449

coordinated chloridion (Cl2) and the hydrogen from C13 (C13—H···Cl2, 2.714 Å). The crystal structures of **2** and **3** show the similar intramolecular hydrogen bond between Cl1 and the proton of C14, C14—H···Cl1, and the lengths are 2.823 and 2.826 Å, respectively.

In the crystal structures of **4**−**6**, the complexes with the acetophenone-N^4-substituent thiosemicarbazone ligands, the same T-stacking (edge-to-face) π-interactions are identified (Figure 4) with regard to the nonbonded interactions between the aromatic rings (distances from 2.478 to 2.840 Å).[21] This is supported by the aforementioned high-field shift of one of the aromatic protons in ^{1}H NMR spectra of **4**−**9** which is likely due to the close vicinity of the phenyl group in the relevant ketone moiety of the coordinated ligand. In the crystal structure of **4**, the lengths of C11−S1 and C11−N2 bonds are 1.687 and 1.342 Å, respectively, which are similar to those of **L4**, consistent with a thioamide (—N—C═S) resonance form of the coordinated ligand (Figure 1). The [(η^6-p-cymene)-Ru^{II}(**L5**)Cl]Cl·CHCl$_3$ (**5**·CHCl$_3$) and [(η^6-p-cymene)-Ru^{II}(**L6**)Cl]Cl·CHCl$_3$ (**6**·CHCl$_3$) crystallized with one molecule of solvent (CHCl$_3$) in the lattice per molecule of complex, respectively. Moreover, the crystal structure of **5**·CHCl$_3$ shows intramolecular H-bonding involving the Cl1 and C15 (C15—H···Cl1 2.781 Å).

In the crystal structure of **9** (Figure 4), the N2 of **L9** ligand is deprotonated, and the complex is neutral. As a consequence of deprotonation, the C11−S1 bonds (formally double bonds in the free **L9** ligand) lengthen from 1.659 to 1.735 Å (Table 2), while the C11−N2 bonds shorten from 1.368 to 1.302 Å; consistent with a dominantly ene-thiolate (—N═C—S—) resonance form of the coordinated ligand (Figure 5). Similar to
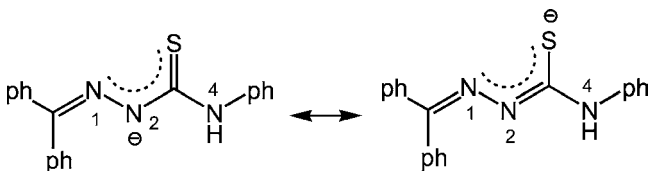

Figure 5. Different resonance form of **L9** with N2-protonated.

the structures of **4**−**6**, one of the benzene rings from the benzophenone system of **L9** in the crystal structure of **9** is pointed toward the p-cymene ligand (Figure 4), which results in the intramolecular CH/π interactions between C7−H protons and the benzene ring [R(1) = C(19)/C(20)/C(21)/C(22)/C(23)/C(24)] (distance 2.601 Å). In addition, dimers formed in the unit cell (Figure 6) through a pair of intermolecular H-bonds between N1−H, C30−H protons of **L9** and the coordinated chloridion of another molecule, with distances 2.674 and 2.805 Å, respectively, and Ru−Cl (2.435 Å) in **9** is slightly longer than that of **1**−**6** (2.398−2.415 Å) owing to the formation of dimers.

Cancer Cell Growth Inhibition. The cytotoxicity of the series of TSC ligands (**L1**−**L9**) and their corresponding [(η^6-p-cymene)Ru^{II}(TSC)Cl]Cl complexes (**1**−**9**) was determined using the MTT assay on human gastric carcinoma (SGC-7901) and human liver carcinoma (BEL-7404) cell lines, and for comparison purposes the cytotoxicity of cisplatin, oxaliplatin, and carboplatin was evaluated under the same experimental conditions (Table 3). The IC$_{50}$ values of the most of the TSC ligands toward these two carcinoma cells are deemed inactive (>100 μM). In the series of TSC ligands, **L3** shows the highest
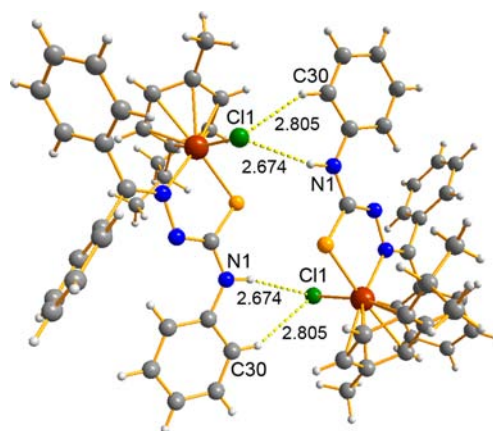

Figure 6. H-bonding involving the coordinated chloridion and the **L9** ligand of [(η^6-p-cymene)Ru^{II}(**L9**)Cl]Cl (**9**) giving rise to dimers in the unit cell.

activity with an IC$_{50}$ value of 39 μM against SGC-7901 carcinoma cell lines, and **L6** displays the highest activity with an IC$_{50}$ value around 37 μM against BEL-7404 carcinoma cell lines. In comparison to their free ligands, the Ru-arene complexes demonstrated significantly increased antiproliferative activity (Table 3). All the complexes exhibit moderate cytotoxicity against the two cancer cell lines, with the IC$_{50}$ values in the micromolar range (16−48 μM). Notably, under the experimental conditions the series of complexes shows comparable activity to cisplatin and oxaliplatin (16−32 μM to ~20 μM), and are more cytotoxic than carboplatin, against BEL-7404 cell line, indicating the good cytotoxicity of these complexes. The compounds with the N^4-substitution of the phenyl ring (**3**, **6**, and **9**), to within experimental errors, appear to have the higher anticancer activity against the two cell lines compared to the H and methyl substituted. This may be due to a structural effect, as the N^4-phenyl can adjust the hydrophobicity of the compound, which may influence the interaction with biological targets as the similar mechanism of action as that for the analogues, [(η^6-arene)Ru(en)Cl]$^+$.[22] However, the type of ketone which condensates to N^1, seems to be of minor importance for the cytotoxic activity. In order to assess selectivity of the compounds for tumor cells rather than normal cell lines, the compounds were also screened for their antiproliferative effects on the human embryonic kidney (HEK-293T, a model for healthy cells) cell lines. In most cases of the compounds, the cytotoxicity is comparable for the tumors and normal cell lines. Compared to the TSC ligands, most of the Ru-arene complexes show relatively high cytotoxicity toward the noncancerous HEK-293T cells, indicating that the complexes are not selective. It is noteworthy that complex **1**, which is markedly more toxic on the tumor cell lines (IC$_{50}$ of ~30 μM) than on the noncancerous HEK-293T cells (IC$_{50}$ of >100 μM), shows the most selectivity for tumor cells rather than normal cell lines in the series of complexes.

It is reported that the Ru-arene complexes containing N,N-,[23] N,O-,[18,24] and O,O-chelating[25] ligands show activity toward some human cancer cells with an IC$_{50}$ value in the submicromolar or micromolar range (0.2−240 μM), and some Ru-arene compounds of the RAPTA type[26] show IC$_{50}$ values from 2 to 49 μM against A2780 human ovarian cancer cells. In addition, the Ru-arene complexes [(arene)$_2$Ru$_2$(SR)$_3$]Cl with IC$_{50}$ values in the nanomolar range (0.03−0.66 μM) are reported,[27] in which the most active complex is more than 100

Table 3. IC$_{50}$ Values of TSCs (L1−L9), Complexes (1−9), Cisplatin, Oxaliplatin, and Carboplatin towards SGC-7901, BEL-7404, and HEK-293T Cell Lines

	IC$_{50}(\mu M)$				IC$_{50}(\mu M)$		
TSC	SGC-7901	BEL-7404	HEK-293T	complex	SGC-7901	BEL-7404	HEK-293T
L1	>100	>100	>100	1	30.8 ± 5.7	32.0 ± 3.1	>100
L2	>100	96.1 ± 9.7	>100	2	39.9 ± 2.6	28.2 ± 0.6	22 ± 3.5
L3	38.6 ± 4.3	>100	97 ± 8.3	3	17.5 ± 1.6	18.2 ± 3.2	25 ± 0.9
L4	62.2 ± 6.1	>100	41 ± 4.1	4	28.6 ± 3.5	29.1 ± 7.1	46 ± 2.5
L5	>100	>100	68 ± 5.9	5	43.4 ± 9.3	29.7 ± 0.5	33 ± 0.4
L6	>100	37.1 ± 0.1	>100	6	46.7 ± 0.6	15.9 ± 2.2	17 ± 4.3
L7	>100	50.1 ± 4.9	51 ± 6.3	7	47.7 ± 1.3	24.5 ± 2.2	20 ± 1.3
L8	>100	>100	>100	8	34.4 ± 3.1	21.8 ± 4.4	17 ± 2.2
L9	>100	45.4 ± 4.1	>100	9	17.0 ± 2.9	17.1 ± 4.6	10 ± 2.0
				cisplatin	6.7 ± 0.4	23.1 ± 2.6	10 ± 0.7
				oxaliplatin	11 ± 0.8	20 ± 0.6	2 ± 0.2
				carboplatin	39 ± 2.6	70 ± 9.5	44 ± 3.7

times more cytotoxic than cisplatin toward A2780 and A2780cisR cells. The *in vitro* anticancer activity of our compounds is moderate compared with the above-reported compounds. However, *in vitro* anticancer potency appears not to be a prerequisite in particular for ruthenium drug candidates;[28] i.e., RAPTA compounds exhibit low activity against cancer cells but possess very good antimetastatic activity *in vivo*.[10]

Biological Assays: Gel Electrophoresis of Compound-*pBR*322 Complexes. As DNA is generally a potential target for arene-ruthenium(II) drugs,[29] it is among the critically important targets in cancer chemotherapy. Most cytotoxic ruthenium drugs act as DNA intercalators upon coordination to the appropriate ancillary ligands.[30] Thus, the interactions of the representative TSC ligands (L1−L3) and their corresponding complexes (1−3) with DNA were investigated. For comparison purposes, plasmid DNA was incubated in presence of the representative TSC ligands (L1−L3) and their corresponding complexes (1−3) for 24 h at 37 °C at the molar ratios (r = 0.4 and 0.8). The cleaving efficiency of all compounds was assessed by their ability to convert supercoiled *pBR*322 DNA (form I) to nicked DNA (form II), while no linear DNA (form III) was observed, by agarose gel electrophoresis (Figure 7). The DNA
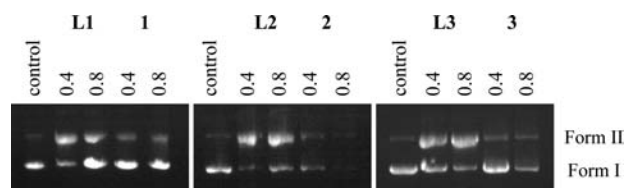

Figure 7. Gel electrophoresis of *pBR*322 plasmid DNA incubated in presence of (from left to right on each gel) the TSC ligands (L1−L3) and their corresponding complexes (1−3) for 24 h at the molar ratios (r = 0.4 and 0.8).

cleaving abilities of complexes (1−3) are in concentration-dependent manners. With increasing concentration of complexes (1−3), the amount of SC DNA (form I) diminishes gradually whereas the NC DNA (form II) exhibits no obvious change. The DNA binding results of these complexes are similar to that of Ru(II)-DMSO-Cl-Chalcone[31] and some other Ru-arene complexes,[29b,32] indicating a similar oxidative mechanism. Surprisingly, the result of agarose gel electrophoresis of TSC ligands (L1−L3) shows a different

phenomenon. A control experiment showed that SC DNA (form I) was cleaved by TSC ligands (L1−L3), and formed NC DNA (form II), indicating a different interaction mode between TSC ligands and DNA.[33] Obviously, the DNA binding activities of the ruthenium complexes are higher than that of TSC ligands, which correlates quite well with their cytotoxicity.

CONCLUSIONS

In conclusion, nine TSC compounds (L1−L9) and their corresponding Ru-arene complexes (1−9) have been synthesized and characterized by a variety of physical methods. The molecular structures of L4, L9, 1−6, and 9 have been characterized by X-ray crystallography. The *in vitro* activity of all the compounds has been evaluated against the SGC-7901 human gastric cancer, BEL-7404 human liver cancer and HEK-293T noncancerous cell lines, and compared to that of cisplatin, oxaliplatin, and carboplatin, the well-known antitumor agents. The TSC compounds exhibited lower antiproliferative activities, but the Ru-arene complexes were found to exhibit moderate activities. Especially, some of the Ru-arene complexes showed IC$_{50}$ cytotoxicity coefficients similar to those of cisplatin and oxaliplatin. Compared to the TSC ligands, most of the Ru-arene complexes show relatively high cytotoxicity toward the noncancerous HEK-293T cells, indicating that the complexes are not selective. The results of agarose gel electrophoresis indicate that the interaction mechanisms with *pBR*322 plasmid DNA are different for the TSC ligands and their corresponding complexes.

ASSOCIATED CONTENT

Ⓢ Supporting Information
Crystallographic data in CIF format. This material is available free of charge via the Internet at http://pubs.acs.org.

AUTHOR INFORMATION

Corresponding Author
*E-mail: suwmail@163.com (W.S.); lipearpear@163.com (P.L.). Phone: + 86 771 3908065.

Notes
The authors declare no competing financial interest.

ACKNOWLEDGMENTS

■ REFERENCES

(1) (a) Beraldo, H.; Gambino, D. *Mini-Rev. Med. Chem.* **2004**, *4*, 31−39. (b) Yu, Y.; Kalinowski, D. S.; Kovacevic, Z.; Siafakas, A. R.; Jansson, P. J.; Stefani, C.; Lovejoy, D. B.; Sharpe, P. C.; Bernhardt, P. V.; Richardson, D. R. *J. Med. Chem.* **2009**, *52*, 5271−5294. (c) Kalinowski, D. S.; Quach, P.; Richardson, D. R. *Future Med. Chem.* **2009**, *1*, 1143−1151.

(2) (a) Ren, S.; Wang, R.; Komatsu, K.; Bonaz-Krause, P.; Zyrianov, Y.; McKenna, C. E.; Csipke, C.; Tokes, Z. A.; Lien, E. J. *J. Med. Chem.* **2002**, *45*, 410−419. (b) Hall, M. D.; Salam, N. K.; Hellawell, J. L.; Fales, H. M.; Kensler, C. B.; Ludwig, J. A.; Szakacs, G.; Hibbs, D. E.; Gottesman, M. M. *J. Med. Chem.* **2009**, *52*, 3191−3204. (c) Hall, M. D.; Brimacombe, K. R.; Varonka, M. S.; Pluchino, K. M.; Monda, J. K.; Li, J.; Walsh, M. J.; Boxer, M. B.; Warren, T. H.; Fales, H. M.; Gottesman, M. M. *J. Med. Chem.* **2011**, *54*, 5878−5889.

(3) (a) Adsule, S.; Barve, V.; Chen, D.; Ahmed, F.; Dou, Q. P.; Padhye, S.; Sarkar, F. H. *J. Med. Chem.* **2006**, *49*, 7242−7246. (b) Kalinowski, D. S.; Yu, Y.; Sharpe, P. C.; Islam, M.; Liao, Y. T.; Lovejoy, D. B.; Kumar, N.; Bernhardt, P. V.; Richardson, D. R. *J. Med. Chem.* **2007**, *50*, 3716−3729. (c) Richardson, D. R.; Kalinowski, D. S.; Richardson, V.; Sharpe, P. C.; Lovejoy, D. B.; Islam, M.; Bernhardt, P. V. *J. Med. Chem.* **2009**, *52*, 1459−1470.

(4) (a) Beckford, F. A.; Leblanc, G.; Thessing, J.; Shaloski, M., Jr.; Frost, B. J.; Li, L.; Seeram, N. P. *Inorg. Chem. Commun.* **2009**, *12*, 1094−1098. (b) Zeglis, B. M.; Divilov, V.; Lewis, J. S. *J. Med. Chem.* **2011**, *54*, 2391−2398.

(5) (a) Hartinger, C. G.; Zorbas-Selfried, S.; Jakupee, M. A.; Kynast, B.; Zorbas, H.; Keppler, B. K. *J. Inorg. Biochem.* **2006**, *100*, 891−904. (b) Yan, Y. K.; Melchart, M.; Habtemariam, A.; Sadler, P. J. *Chem. Commun.* **2005**, 4764−4776. (c) Hotze, A. C. G.; Kariuki, B. M.; Hannon, M. J. *Angew. Chem.* **2006**, *118*, 4957−4960. (d) Vajpayee, V.; Yang, Y. J.; Kang, S. C.; Kim, H.; Kim, I. S.; Wang, M.; Stang, P. J.; Chi, K.-W. *Chem. Commun.* **2011**, *47*, 5184−5186.

(6) (a) Rademaker-Lakhai, J. M.; Van Den Bongard, D.; Pluim, D.; Beijnen, J. H.; Schellens, J. H. M. *Clin. Cancer Res.* **2004**, *10*, 3717−3727. (b) Hartinger, C. G.; Jakupec, M. A.; Zorbas-Seifried, S.; Groessl, M.; Egger, A.; Berger, W.; Zorbas, H.; Dyson, P. J.; Keppler, B. K. *Chem. Biodiversity* **2008**, *5*, 2140−2155. (c) Suess-Fink, G. *Dalton Trans.* **2010**, *39*, 1673−1688.

(7) (a) Hartinger, C. G.; Dyson, P. J. *Chem. Soc. Rev.* **2009**, *38*, 391−401. (b) Kurzwernhart, A.; Kandioller, W.; Bächler, S.; Bartel, C.; Martic, S.; Buczkowska, M.; Mühlgassner, G.; Jakupec, M. A.; Kraatz, H.-B.; Bednarski, P. J.; Arion, V. B.; Marko, D.; Keppler, B. K.; Hartinger, C. G. *J. Med. Chem.* **2012**, *55*, 10512−10522. (c) Romero-Canelón, I.; Salassa, L.; Sadler, P. J. *J. Med. Chem.* **2013**, *56*, 1291−1300.

(8) (a) Smith, G. S.; Therrien, B. *Dalton Trans.* **2011**, *40*, 10793−10800. (b) Kurzwernhart, A.; Kandioller, W.; Enyedy, É. A.; Novak, M.; Jakupec, M. A.; Keppler, B. K.; Hartinger, C. G. *Dalton Trans.* **2011**, *42*, 6193−6202.

(9) (a) Chen, H.; Parkinson, J. A.; Parsons, S.; Coxall, R. A.; Gould, R. O.; Sadler, P. J. *J. Am. Chem. Soc.* **2002**, *124*, 3064−3082. (b) Liu, H.-K.; Wang, F.; Parkinson, J. A.; Bella, J.; Sadler, P. J. *Chem.—Eur. J.* **2006**, *12*, 6151−6165.

(10) (a) Scolaro, C.; Bergamo, A.; Brescacin, L.; Delfino, R.; Cocchietto, M.; Laurenczy, G.; Geldbach, T. J.; Sava, G.; Dyson, P. J. *J. Med. Chem.* **2005**, *48*, 4161−4171. (b) Chatterjee, S.; Kundu, S.; Bhattacharyya, A.; Hartinger, C. G.; Dyson, P. J. *JBIC, J. Biol. Inorg. Chem.* **2008**, *13*, 1149−1155.

(11) Beckford, F.; Dourth, D.; Shaloski, M., Jr.; Didion, J.; Thessing, J.; Woods, J.; Crowell, V.; Gerasimchuk, N.; Gonzalez-Sarrías, A.; Seeram, N. P. *J. Inorg. Biochem.* **2011**, *105*, 1019−1029.

(12) (a) Stringer, T.; Therrien, B.; Hendricks, D. T.; Guzgay, H.; Smith, G. S. *Inorg. Chem. Commun.* **2011**, *14*, 956−960. (b) Adams, M.; Li, Y.; Khot, H.; De Kock, C.; Smith, P. J.; Land, K.; Chibalea, K.; Smith, G. S. *Dalton Trans.* **2013**, *42*, 4677−4685.

(13) (a) Demoro, B.; Sarniguet, C.; Sanchez-Delgado, R.; Rossi, M.; Liebowitz, D.; Caruso, F.; Olea-Azar, C.; Moreno, V.; Medeiros, A.; Comini, M. A.; Otero, L.; Gambino, D. *Dalton Trans.* **2012**, *41*, 1535−1543. (b) Demoro, B.; de Almeida, R. F. M.; Marques, F.; Matos, C. P.; Otero, L.; Pessoa, J. C.; Santos, I.; Rodríguez, A.; Moreno, V.; Lorenzo, J.; Gambino, D.; Tomaz, A. I. *Dalton Trans.* **2013**, *42*, 7131−7146.

(14) *SAINT Software Reference Manual*; Bruker AXS: Madison, WI, 1998.

(15) Sheldrick, G. M. *Acta Crystallogr.* **1990**, *A46*, 467.

(16) Sheldrick, G. M. *SHELXS-97, Program for X-ray Crystal Structure Solution*; University of Göttingen: Göttingen, Germany, 1997.

(17) (a) Peacock, A. F. A.; Melchart, M.; Deeth, R. J.; Habtemariam, A.; Parsons, S.; Sadler, P. J. *Chem.—Eur. J.* **2007**, *13*, 2601−2613. (b) Fernandez, R.; Melchart, M.; Habtemariam, A.; Parsons, S.; Sadler, P. J. *Chem.—Eur. J.* **2004**, *10*, 5173−5179.

(18) Pettinari, R.; Pettinari, C.; Marchetti, F.; Clavel, C. M.; Scopelliti, R.; Dyson, P. J. *Organometallics* **2013**, *32*, 309−316.

(19) (a) Palenik, G. J.; Rendle, D. F.; Carter, W. S. *Acta Crystallogr.* **1974**, *B30*, 2390−2395. (b) Parsons, S.; Smith, A. G.; Tasker, P. A.; White, D. J. *Acta Crystallogr., Sect. C* **2000**, *C56*, 237−238. (c) Jian, F.; Bai, Z.; Xiao, H.; Li, K. *Acta Crystallogr., Sect. E* **2005**, *E61*, o653−o654. (d) Venkatraman, R.; Ameera, H.; Sitole, L.; Ells, E.; Fronczek, F. R.; Valente, E. J. *J. Chem. Crystallogr.* **2009**, *39*, 711−718. (e) Jian, F.; Li, Y.; Xiao, H. *Acta Crystallogr., Sect. E* **2005**, *E61*, o2219−o2220. (f) Lobana, T. S.; Khanna, S.; Butcher, R. J.; Hunter, A. D.; Zeller, M. *Polyhedron* **2006**, *25*, 2755−2763.

(20) Richardson, D. R.; Kalinowski, D. S.; Richardson, V.; Sharpe, P. C.; Lovejoy, D. B.; Islam, M.; Bernhardt, P. V. *J. Med. Chem.* **2009**, *52*, 1459−1470.

(21) (a) Sinnokrot, M. O.; Sherrill, C. D. *J. Am. Chem. Soc.* **2004**, *126*, 7690−7697. (b) Catak, S.; D'hooghe, M.; De Kimpe, N.; Waroquier, M.; Van Speybroeck, V. *J. Org. Chem.* **2010**, *75*, 885−896.

(22) Aird, R. E.; Cummings, J.; Ritchie, A. A.; Muir, M.; Morris, R. E.; Chen, H.; Sadler, P. J.; Jodrell, D. I. *Br. J. Cancer* **2002**, *86*, 1652−1657.

(23) Filak, L. K.; Muhlgassner, G.; Bacher, F.; Roller, A.; Galanski, M.; Jakupec, M. A.; Keppler, B. K.; Arion, V. B. *Organometallics* **2011**, *30*, 273−283.

(24) van Rijt, S.; Hebden, A.; Amaresekera, T.; Deeth, R.; Clarkson, G.; Parsons, S.; McGowan, P.; Sadler, P. *J. Med. Chem.* **2009**, *52*, 7753−7764.

(25) (a) Turel, I.; Kljun, J.; Perdih, F.; Morozova, E.; Bakulev, V.; Kasyanenko, N.; Byl, J. A.; Osheroff, N. *Inorg. Chem.* **2010**, *49*, 10750−10752. (b) Kandioller, W.; Hartinger, C. G.; Nazarov, A. A.; Bartel, C.; Skocic, M.; Jakupec, M. A.; Arion, V. B.; Keppler, B. K. *Chem.—Eur. J* **2009**, *15*, 12283−12291. (c) Hanif, M.; Meier, S. M.; Kandioller, W.; Bytzek, A.; Hejl, M.; Hartinger, C. G.; Nazarov, A. A.; Arion, V. B.; Jakupec, M. A.; Dyson, P. J.; Keppler, B. K. *J. Inorg. Biochem.* **2011**, *105*, 224−231.

(26) (a) Dutta, B.; Scolaro, C.; Scopelliti, R.; Dyson, P. J.; Severin, K. *Organometallics* **2008**, *27*, 1355−1357. (b) Kilpin, K. J.; Clavel, C. M.; Edafe, F.; Dyson, P. J. *Organometallics* **2012**, *31*, 7031−7039.

(27) (a) Giannini, F.; Furrer, J.; Ibao, A.-F.; Süss-Fink, G.; Therrien, B.; Zava, O.; Baquie, M.; Dyson, P. J.; Stepnicka, P. *JBIC, J. Biol. Inorg. Chem.* **2012**, *17*, 951−960. (b) Ibao, A.-F.; Gras, M.; Therrien, B.; Süss-Fink, G.; Zava, O.; Dyson, P. J. *Eur. J. Inorg. Chem.* **2012**, 1531−1535.

(28) Hanif, M.; Henke, H.; Meier, S. M.; Martic, S.; Labib, M.; Kandioller, W.; Jakupec, M. A.; Arion, V. B.; Kraatz, H. B.; Keppler, B. K.; Hartinger, C. G. *Inorg. Chem.* **2010**, *49*, 7953−7963.

(29) (a) Wang, F.; Bella, J.; Parkinson, J. A.; Sadler, P. J. *JBIC, J. Biol. Inorg. Chem.* **2005**, *10*, 147−155. (b) Govender, P.; Renfrew, A. K.; Clavel, C. M.; Dyson, P. J.; Therrienc, B.; Smith, G. S. *Dalton Trans.* **2011**, *40*, 1158−1167.

(30) (a) Liu, H. K.; Berners-Price, S. J.; Wang, F. Y.; Parkinson, J. A.; Xu, J. J.; Bella, J.; Sadler, P. J. *Angew. Chem., Int. Ed.* **2006**, *45*, 8153−8156. (b) Liu, H.-K.; Sadler, P. *Acc. Chem. Res.* **2011**, *44*, 349−359.

(c) Chen, H.; Parkinson, J. A.; Parsons, S.; Coxall, R. A.; Gould, R. O.; Sadler, P. J. *J. Am. Chem. Soc.* **2002**, *124*, 3064−3082. (d) Chen, H.; Parkinson, J. A.; Morris, R. E.; Sadler, P. J. *J. Am. Chem. Soc.* **2003**, *125*, 173−186. (e) Zeglis, B. M.; Pierre, V. C.; Barton, J. K. *Chem. Commun.* **2007**, 4565−4579.

(31) (a) Bhat, S. S.; Kumbhar, A. A.; Heptullah, H.; Khan, A. A.; Gobre, V. V.; Gejji, S. P.; Puranik, V. G. *Inorg. Chem.* **2011**, *50*, 545−558. (b) Gaur, R.; Mishra, L. *Inorg. Chem.* **2012**, *51*, 3059−3070.

(32) Bugarcic, T.; Novakova, O.; Halamikova, A.; Zerzankova, L.; Vrana, O.; Kasparkova, J.; Habtemariam, A.; Parsons, S.; Sadler, P. J.; Brabec, V. *J. Med. Chem.* **2008**, *51*, 5310−5319.

(33) Huang, H.; Chen, Q.; Ku, X.; Meng, L.; Lin, L.; Wang, X.; Zhu, C.; Wang, Y.; Chen, Z.; Li, M.; Jiang, H.; Chen, K.; Ding, J.; Liu, H. *J. Med. Chem.* **2010**, *53*, 3048−3064.